COBEM 2021 26th International Congress of Mechanical Engineering
November 22-26, 2021, Virtual Congress, Brazil
ABCM Associação Brasileira de Engenharia e Ciências Mecânicas

COB-2021-XXXX
FINITE ELEMENT ANALYSIS ON BIOFUEL PARTICLES DISPERSION

João P. I. Souza
Gustavo R. Anjos
COPPE/Department of Mechanical Engineering, Federal University of Rio de Janeiro, Brazil
jpisouza@mecanica.coppe.ufrj.br, gustavo.rabello@coppe.ufrj.br

Abstract. *Particle-laden multiphase flow is an important subject of study in fluid mechanics. In this work, the particle emission from biofuel production and storage is analyzed and simulated, with respect to the different geometries associated with the fluid dynamics and dispersion of said pollutants, in order to obtain the main effects of such transportation into the atmosphere, that may cause environmental and health damages. The continuous phase is numerically simulated through the Navier-Stokes equations, for which the results are in complete accordance to the ones presented in the literature. As for the solid dispersion, an Euler-Lagrange analysis is made, which provides a better understanding of each particle trajectory. A numerical and optimized simulator is completely built by means of the Finite Element Method (FEM) and the results are obtained for different geometries. A validation of the model is first made with a classical fluid mechanics problem: the lid driven cavity, for both quadratic and MINI interpolations. A second domain is simulated to analyze particles' interaction with a fluid expansion and also with heat transfer is introduced to the problem. All the results and comparisons are shown and discussed throughout this document.*

Keywords: *CFD, FEM, multiphase, particles, biofuel*

1. INTRODUCTION

Biofuel is characterized as an energy source produced from biomass, opposed to those originated from geological processes, called fossil fuels. According to Reham *et al.* (2015), diesel, gasoline and natural gas are among the most commonly used fuels in the past few years. As stated by NASA (2021), fossil fuels are responsible for serious environmental changes, including the increase on global surface temperature. Following the same idea, Xu *et al.* (2018) defend that developing fuel from renewable sources, and not from fossil ones, has become an urgent matter, which led to government regulations and stringent laws on greehouse gas reductions, as presented by Hashim *et al.* (2016).

An important result shown by Kim *et al.* (2015) is that the net indicated efficiency of a spark ignition (SI) engine can be increased by 4.0% when ethanol is added to gasoline. Also, Kim *et al.* (2015) show the correlation between the type of mixture ethanol+gasoline and the particle emission. Also the particle size spectra for three different types of gasoline+ethanol mixtures is shown.

Still in the topic of pollution and emissions, one of the findings by Hashim *et al.* (2016) is that, when comparing different biofuel blends with Diesel, it is of easy conclusion that a minimum of 20% reduction on CO_2 emission is observed between the first and the second ones.

In the fluid mechanics field of study, the Navier-Stokes equations are cue formulation to be studied, as seen in Batchelor (2000), along with the continuity equation. As can be noticed, this set of equations, in spite of being a powerful way of characterizing the behavior of any sort of flow, has a complex form, mainly due to its non-linearity, with respect to velocity variables. Given that most common cases may not be simplified without considerable loss of information and representativeness of the phenomenon, numerical solutions are required.

Zienkiewicz and Taylor (2000) published a volume of his collection dedicated to fluid mechanics' equation solving by means of the Finite Element Method. One possible approach, also used by Abdelwahed *et al.* (2011), makes use of the stream function (ψ) and vorticity (ω) formulation, modifying the set of equations to the vorticity form, eliminating pressure gradient dependence. Said correlation is also presented by da Cunha (2020).

Alternatively, Bagai *et al.* (2020) use the stream function-vorticity approach as well but, instead of the finite element method for the numerical solution, the authors use the finite difference approximation for the derivatives. The problem examined to validate the method is the four-sided lid driven cavity, with heat and mass transfer coupled to the fluid mechanics problem.

The results presented by the authors in their articles are satisfying in terms of showing the method used is adequate. Abdelwahed *et al.* (2011) compare their method with the exact solution of the quasi-Stokes problem, as shown in the document. The authors compare graphically both solutions, which makes evident how similar and accurate the numerical solution is to the exact one, and plot the total error associated to the simulation, concluding that many engineering

problems related to the Navier-Stokes equations can be solved by means of this technique. Bagai *et al.* (2020) validate the four-sided lid driven cavity with values found in the literature, resulting in the plot found in the article, where the literature points are confronted with simulated results, showing that the simulated points are very close to the reference. The validation is made for a Reynolds number of 100, with velocity in both horizontal and vertical directions. Besides, the center of vortices are compared to two other literature sources, for three different Reynolds numbers, with satisfying results. The work also presents interesting streamline contour and vorticity plots to illustrate the example solved. Zhang *et al.* (2018) validate their results with the exact solution and ANSYS Fluent solution. The comparison is presented in the form of a plot as well, where simulated points are extremely close to the analytical solution, for different values of k. da Cunha (2020) provides a relevant validation of the lid-driven cavity problem, comparing with the literature, for different Reynolds number, showing that the Stream function-Vorticity formulation generates accurate results. The author also shows graphical results of the flow around a cylinder and the oscillation of the drag force.

The different methods presented in this section are well-known methods for computational fluid mechanics problems. After presenting their results, the next step is to analyze the different approaches to multiphase flow simulation, which is an important aspect in biofuel particle emission analysis. The next step is to couple fluid mechanics study with particles subjected to drag and lift in a flow, analyzing and evaluating methods for such simulation, going through mathematical models that describe and characterize all relevant aspects and phenomena in the fluid-particle interaction.

When solid-liquid mixtures are studied, researchers often come across separation methods, such as centrifuge, cyclones or hydrocyclones. Hoffmann *et al.* (2019) state in their work the importance of hydrocyclones and provides an investigation of its acting on liquids of varying viscosity. Hoffmann *et al.* (2019) offer both numerical and experimental analyses of particle trajectories inside the equipment, which, as described by them, are unexpected. The simulation type used is the large-eddy one (LES). This work is particularly interesting because it denotes a centrifugal flow, where the centrifugal force has great influence on the behavior of particle trajectories.

Another approach on multiphase flow simulation is presented by Barghi (2015), by means of the commercial package ANSYS-Fluent. The main fluid is air and was modeled with the $\kappa-\epsilon$ model, which is of great importance on turbulent flow study and the values of κ and ϵ are calculated by Barghi (2015) through transport equations. For droplet/particle motion an Euler-Lagrange approach is used. Borello *et al.* (2012) also provide the kinetic energy equation for the particles that hit the walls in the simulated body. It is an interesting discussion since many particles may be retained through adhesion in the walls and can lead equipments to failure.

Greifzu *et al.* (2015) present a good comparison between the commercial software ANSYS and OpenFOAM's open source solvers for Euler-Lagrange models using RANS simulation. As observed, ANSYS uses the Shiller and Naumann expression seen in Borello *et al.* (2012) and Barghi (2015). OpenFOAM, however has an alternative and slightly different expression for spherical bodies, as seen in Greifzu *et al.* (2015). Barghi (2015) validated the code by comparing the prill sizes of both measured and CFD analyses, resulting in values of same order. Hoffmann *et al.* (2019) showed an interesting comparison between particle tracks obtained from the camera and the simulated trajectories. Both images are interestingly similar, validating the simulated results. The authors also presented a plot for axial velocity against radial position, confirming that particles and fluid that are closer to the center move upwards (to the overflow exit) and the ones that are closer to the walls, and therefore have a higher density, move downwards. Borello *et al.* (2012) also validated their adhesion model through a real experiment comparison. Adhesion field images are shown next to experiment photos, which were executed under the same conditions for compressor blades. One interesting conclusion is that most deposits were induced by the presence of large recirculation. The validation shown by Greifzu *et al.* (2015) is important to prove the effectiveness of OpenFOAM's solvers, when compared to ANSYS's well known Fluent software.

The present work is intended to analyze numerical simulation of multiphase flows under several circumstances. As simulation method, the Finite Element Analysis (FEA) will be used. Particle motion will be determined by an Euler-Lagrange approach, where the continuous phase, in contact to every single solid body, exercises forces that can be placed in two main categories: drag and buoyancy.

2. GOVERNING EQUATIONS OF THE FLUID AND SOLID PHASES

2.1 The Continuous Phase

The governing equation for an incompressible fluid phase in its vectorial form is given by equation 1, known as the Navier-Stokes equation, as presented by Batchelor (2000).

$$\frac{\partial \mathbf{u}}{\partial t} + \mathbf{u} \cdot \nabla \mathbf{u} - \nu \nabla^2 \mathbf{u} + \frac{1}{\rho} \nabla p = \mathbf{g} \tag{1}$$

Here $\mathbf{u}$ is the velocity vector, p the pressure and ν the kinematic viscosity. g is a field source term, generally representing gravitational field. The non-dimensional variables for cases where a characteristic velocity U is identified, such as an

expansion, are calculated as follows, where the subscript D indicates the dimensional variable:

$$\mathbf{x} = \frac{\mathbf{x}_D}{L}, \quad \mathbf{u} = \frac{\mathbf{u}_D}{U}, \quad t = \frac{t_D U}{L}, \quad \mathbf{g} = \frac{\mathbf{g}_D}{|\mathbf{g}_{ref}|}, \quad p = \frac{p_D}{\rho U^2} \tag{2}$$

Replacing the dimensional values by correlations (2), one may find the continuity and the momentum equation in non-dimensional form as follows:

$$\nabla \cdot \mathbf{u} = 0 \tag{3}$$

$$\frac{\partial \mathbf{u}}{\partial t} + \mathbf{u} \cdot \nabla \mathbf{u} = -\nabla p + \frac{1}{Re}\nabla^2 \mathbf{u} + \frac{1}{Fr^2}\mathbf{g} \tag{4}$$

$Re = UL/\nu$ is known as the Reynolds number and $Fr = U/\sqrt{gL}$ the Froude number. In addition, for the cases where the characteristic velocity U is not known and there is a temperature gradient ΔT responsible for convective flow, the non-dimensional form of $\mathbf{u}$, t, T and p are given as:

$$\mathbf{u} = \frac{\mathbf{u}_D L}{\nu}, \quad t = \frac{t_D \nu}{L^2} \quad T = \frac{T_D}{\Delta T}, \quad p = \frac{p_D L^2}{\rho \nu^2} \tag{5}$$

Using equation 5, one may find the non-dimensional form of the continuity and momentum equation for buoyancy dominant effect, where T is the temperature, as:

$$\frac{\partial \mathbf{u}}{\partial t} + \mathbf{u} \cdot \nabla \mathbf{u} = -\nabla p + \nabla^2 \mathbf{u} + (Ga - GrT)\mathbf{g} \tag{6}$$

Here $Ga = gL^3/\nu^2$ is the Galileo number and $Gr = gL^3\beta\Delta T/\nu^2$ the Grashof number, with β representing the coefficient of thermal expansion. Then, the generic governing equation for an incompressible fluid phase in its vectorial and non-dimensional form is given by equation (1), for which the non-dimensional numbers can be adapted for each case, making $Re = 1.0$ for the convective case and $Ga = 1/Fr^2, Gr = 0$, for the expansion one.

2.2 The Solid Phase

Particles' motion is modeled through the Lagrangian approach, as shown by Crowe *et al.* (2012), given by equation 7, in the non-dimensional form, where all the geometric parameters, variables and properties are nondimensionalized with respect to the ones in the continuous phase.

$$m_p \frac{d\mathbf{u}_p}{dt} = \frac{1}{2} C_D \rho_f A_p |\mathbf{u}_p - \mathbf{u}_f|(\mathbf{u}_p - \mathbf{u}_f) + Ga\frac{\pi}{6}D^3(\rho_p - \rho_f)\mathbf{g} \tag{7}$$

The correlation above consists of Newton's Second Law of motion for the particle subjected to forces made by the flow (drag and buoyancy) and gravity. It is evident that the first term on the right hand side of the equation accounts for drag effects and the second for buoyancy and gravity. The drag coefficient is given by the Shiller and Naumann expression:

$$C_D = \frac{24}{Re_p}\left(1 + 0.14Re_p^{0.687}\right) \tag{8}$$

Where the particle's Reynolds number is defined as a function of the continuous phase's Reynolds number (Re), written as follows:

$$Re_p = Re\frac{\rho_f D_p|\mathbf{u}_p - \mathbf{u}_f|}{\mu} \tag{9}$$

The subscripts p and f refer to particle and fluid, respectively, and m, A and D are the particle's mass, section Area and diameter, in that order.

3. THE FINITE ELEMENT METHOD

3.1 The Variational Form

According to Zienkiewicz and Taylor (2000), the weak form, also known as variational form, is obtained by multiplying each of the governing equation by the weight functions w, q and r, associated with velocity, pressure and temperature, respectively.

$$\int_\Omega \frac{D\mathbf{u}}{Dt}\cdot\mathbf{w}d\Omega = -\int_\Omega \nabla p\cdot\mathbf{w}d\Omega + \frac{1}{Re}\int_\Omega\left(\nabla^2\mathbf{u}\right)\cdot\mathbf{w}d\Omega + \int_\Omega Ga\mathbf{g}\cdot\mathbf{w}d\Omega - \int_\Omega GrT\mathbf{g}\cdot\mathbf{w}d\Omega \tag{10}$$

$$\int_\Omega \frac{du}{dx}qd\Omega + \int_\Omega \frac{dv}{dy}qd\Omega = 0 \tag{11}$$

$$\int_\Omega \frac{DT}{Dt}rd\Omega = \frac{1}{RePr}\int_\Omega\left(\nabla^2 T\right)rd\Omega \tag{12}$$

The Green theorem is applied to the second order and pressure gradient terms. Since, in this work, all boundary conditions are either Dirichlet or null Neumann, the boundary integral resulted from such theorem is null and the final variational form is given by:

$$\int_\Omega \frac{D\mathbf{u}}{Dt}\cdot\mathbf{w}d\Omega = \int_\Omega p\nabla\cdot\mathbf{w}d\Omega - \frac{1}{Re}\int_\Omega\left(\nabla\mathbf{u}:\nabla\mathbf{w}\right)d\Omega + \int_\Omega Ga\mathbf{g}\cdot\mathbf{w}d\Omega - \int_\Omega GrT\mathbf{g}\cdot\mathbf{w}d\Omega \tag{13}$$

$$\int_\Omega \frac{du}{dx}wd\Omega + \int_\Omega \frac{dv}{dy}wd\Omega = 0 \tag{14}$$

$$\int_\Omega \frac{DT}{Dt}wd\Omega = -\frac{1}{RePr}\int_\Omega\left(\nabla T\cdot\nabla w\right)d\Omega \tag{15}$$

3.2 The Galerkin Method

The Galerkin Method consists of an approximation of the continuous variable to a discrete representation. Then, the shape functions N are used, in order to interpolate the values in the nodes seen in Figure 1, where i and j are the global number of the point, corresponding to the local value k.

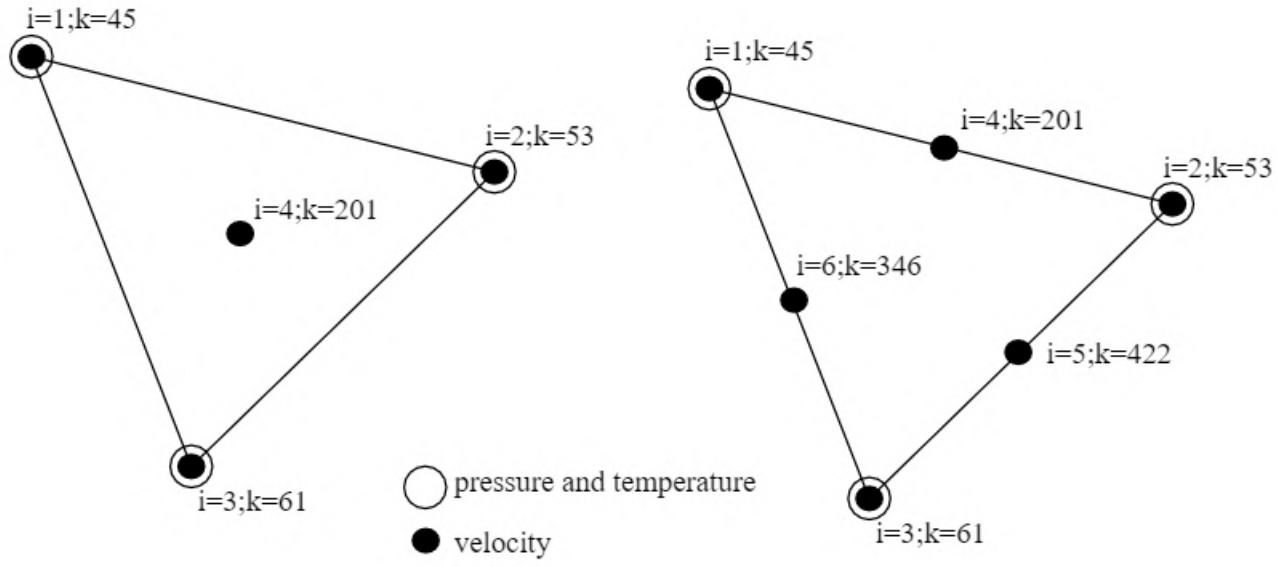

Figure 1: Element's nodes representation, with local (i) and respective global (k) numbers, for MINI (left) and quadratic (right) elements.

Given the elements, the entire mesh is composed by a set of triangular elements, with a total of NP points, for which the velocities u and v are calculated, and NV vertices, where pressure and temperature are associated (therefore a linear interpolation is used for the last two). Both shown elements satisfy the LBB condition and the difference between NV and NP is that NV does not account for the centroid, in the case of the MINI element, and midpoints, for the quadratic ones, seen in Figure 1. For each element, the variables and weight functions may be approximated by the MINI/quadratic shape functions N_i and the linear ones L_i. The N_i interpolation shape functions vary from one element to the other, so that the MINI configuration has 4 N shape functions and the quadratic, 6, which consist of quadratic interpolation functions, both classified within the Taylor-Hood family of finite elements.

$$u \approx \sum_{i=1}^{NP} N_i(x,y)u_i, \quad v \approx \sum_{i=1}^{NP} N_i(x,y)v_i, \quad p \approx \sum_{i=1}^{NV} L_i(x,y)p_i, \quad T \approx \sum_{i=1}^{NV} L_i(x,y)T_i \tag{16}$$

$$\mathbf{w} \approx \sum_{j=1}^{NP} N_j(x,y)\mathbf{w}_j, \quad q \approx \sum_{j=1}^{NV} L_j(x,y)q_j, \quad r \approx \sum_{j=1}^{NV} L_j(x,y)r_j \tag{17}$$

Therefore, the elements used in this work satisfy the Ladyzhenskaya–Babuška–Brezzi (LBB) condition, (Anjos, 2007), so that no artificial stability is included in the Navier-Stokes equations. Substituting the approximated variables, as well as the weight w approximated form, into the governing equations and using the index notation leads to:

$$\sum_e \int_{\Omega_e} \frac{DN_i u_i}{Dt} N_j w_{x_j} d\Omega - \sum_e \int_{\Omega_e} \frac{\partial N_i w_{x_i}}{\partial x} L_j p_j d\Omega + \frac{1}{Re} \sum_e \int_{\Omega_e} \left(\nabla N_i u_i \cdot \nabla N_j w_{x_j}\right) d\Omega$$
$$- \sum_e \int_{\Omega_e} GaN_i g_{x_i} N_j w_{x_j} d\Omega + \sum_e \int_{\Omega_e} GrN_i T_i^+ g_x N_j w_{x_j} d\Omega = 0 \tag{18}$$

$$\sum_e \int_{\Omega_e} \frac{DN_i v_i}{Dt} N_j w_{y_j} d\Omega - \sum_e \int_{\Omega_e} \frac{\partial N_i w_{y_i}}{\partial y} L_j p_j d\Omega + \frac{1}{Re} \sum_e \int_{\Omega_e} \left(\nabla N_i v_i \cdot \nabla N_j w_{y_j}\right) d\Omega - \sum_e \int_{\Omega_e} GaN_i g_{y_i} N_j w_{y_j} d\Omega + \sum_e \int_{\Omega_e} GrN_i T_i^+ g_y N_j w_{y_j} d\Omega = 0 \quad (19)$$

$$\sum_e \left(\int_{\Omega_e} L_i q_i \frac{\partial N_j u_j}{\partial x} d\Omega + \int_{\Omega_e} L_i q_i \frac{\partial N_j v_j}{\partial y} d\Omega \right) = 0 \quad (20)$$

$$\sum_e \left(\int_{\Omega_e} \frac{DL_i T_i}{Dt} L_j r_j d\Omega + \frac{1}{RePr} \int_{\Omega_e} \left(\nabla L_i T_i \cdot \nabla L_j r_j\right) d\Omega \right) = 0 \quad (21)$$

The term T^+ stands for the temperature extended to the centroids of the elements. Since w_j appears on both sides of all the equations, it may be eliminated. Grouping and rearranging the terms, the matrices of the linear systems are presented as follows.

$$M_{ij} = \sum_e \left(\int_{\Omega_e} N_i N_j d\Omega \right), \quad K_{ij} = \sum_e \left(\int_{\Omega_e} \nabla N_i \cdot \nabla N_j d\Omega \right) \quad (22)$$

$$G_{x_{ij}} = \sum_e \left(\int_{\Omega_e} \frac{\partial N_i}{\partial x} L_j d\Omega \right), \quad G_{y_{ij}} = \sum_e \left(\int_{\Omega_e} \frac{\partial N_i}{\partial y} L_j d\Omega \right) \quad (23)$$

$$M^*_{ij} = \sum_e \left(\int_{\Omega_e} L_i L_j d\Omega \right), \quad K^*_{ij} = \sum_e \left(\int_{\Omega_e} \nabla L_i \cdot \nabla L_j d\Omega \right) \quad (24)$$

Finally, the coupled linear system for pressure and velocity may be written:

$$\{\mathbf{M}\} \frac{D\{\mathbf{u}\}}{Dt} + \frac{1}{Re} \{\mathbf{K}\}\{\mathbf{u}\} - \{\mathbf{G}_x\}\{\mathbf{p}\} = Ga\{\mathbf{M}\}\{\mathbf{g}_x\} - Gr\{\mathbf{M}\}\{\mathbf{T}^+\} g_x \quad (25)$$

$$\{\mathbf{M}\} \frac{D\{\mathbf{v}\}}{Dt} + \frac{1}{Re} \{\mathbf{K}\}\{\mathbf{v}\} - \{\mathbf{G}_y\}\{\mathbf{p}\} = Ga\{\mathbf{M}\}\{\mathbf{g}_y\} - Gr\{\mathbf{M}\}\{\mathbf{T}^+\} g_y \quad (26)$$

$$\{\mathbf{D}_x\}\{\mathbf{u}\} + \{\mathbf{D}_y\}\{\mathbf{v}\} = 0 \quad (27)$$

Where $\mathbf{D}_x = \mathbf{G}_x^T$ and $\mathbf{D}_y = \mathbf{G}_y^T$. The temperature is calculated from a separate linear system, as follows:

$$\{\mathbf{M}^*\} \frac{D\{\mathbf{T}\}}{Dt} + \frac{1}{RePr} \{\mathbf{K}^*\}\{\mathbf{T}\} = 0 \quad (28)$$

4. THE SEMI-LAGRANGIAN FORMULATION

After discretizing the spacial derivatives through the finite element method, time derivatives must be discretized as well. Since the material derivative of the velocity results in a non-linear term, a lagrangian approach for that term is used, considering a generic variable ψ, that can either be u, v or T. The Lagrangian formulation is, then:

$$\frac{D\psi}{Dt} \approx \frac{\psi - \psi_d}{\Delta t} \tag{29}$$

Where the subscript d denotes the variable's value at the previous time step in the location the fluid particle occupied (x_d) at that time. Figure 2 explicits how the semi-lagrangian method is made and shows an example of mesh used in this method.

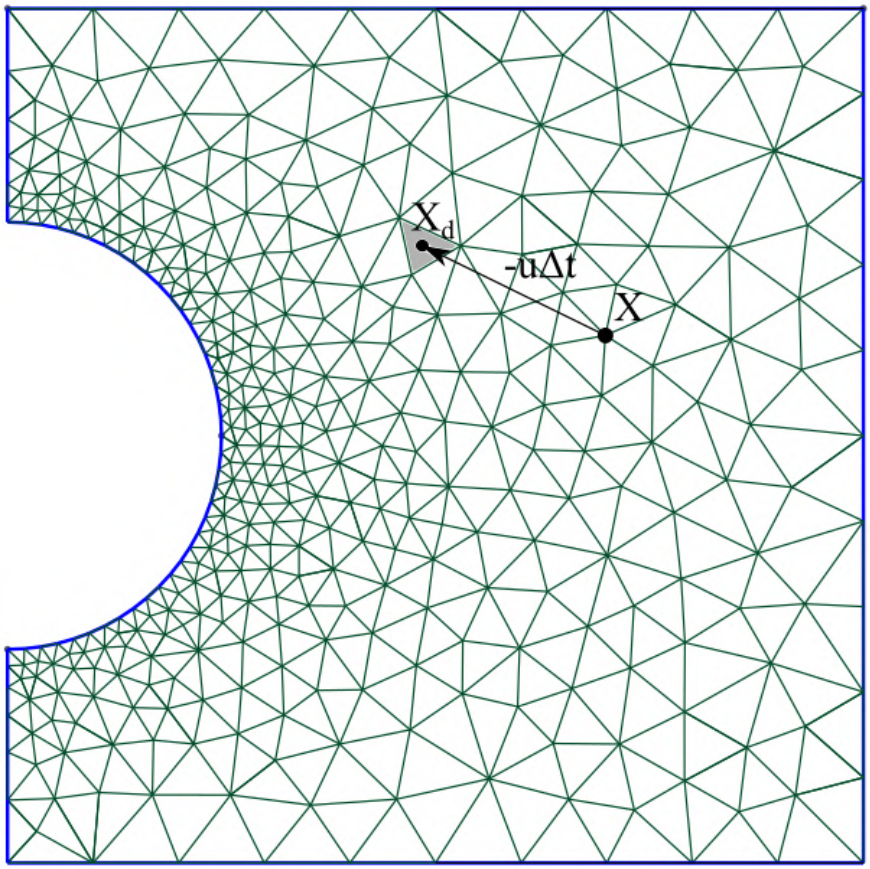

Figure 2: Mesh example and schematic of the semi-lagrangian formulation, where $\mathbf{X}_d$ is the position the fluid particle occupied at the previous time, determined by means of the velocity **u** and the time step Δt.

After determining the position $\mathbf{x}_d = \mathbf{x} - \mathbf{u}\Delta t$ of each point in the mesh, including the centroids/midpoints, the variables u_d, v_d and T_d are calculated by means of the interpolation of such variable's value in the points of the element.

5. RESULTS

5.1 The Lid-driven Cavity

This common CFD problem consists in a cavity, where the upper boundary moves with constant horizontal velocity. This induces a velocity field along the cavity, as can be seen in Figure 3, for $Re = 100$. For this case $Gr = 0$ and $Ga = 1/Fr^2 = 10^{-4}$, where $Fr = U/\sqrt{gL}$ is the Froude number. The mesh used has 3124 elements and 1563 vertices.

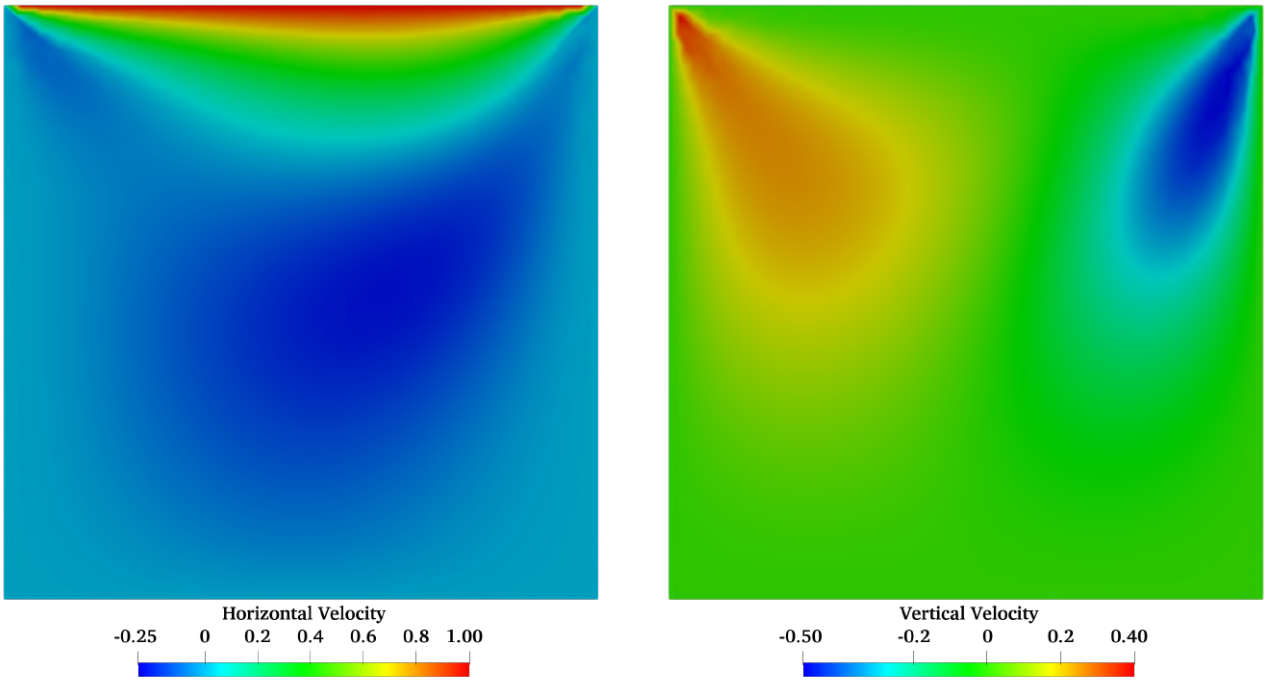

(a) (b)

Figure 3: Velocity fields in the (a) horizontal and (b) vertical directions for the lid-driven cavity problem, for $Re = 100$.

The velocity fields along the vertical and horizontal lines that passe through the midpoint of the square domain are compared to the results seen in da Cunha (2020). Figure 4 shows the comparison between the current work and the literature, for the MINI and the quadratic formulations.

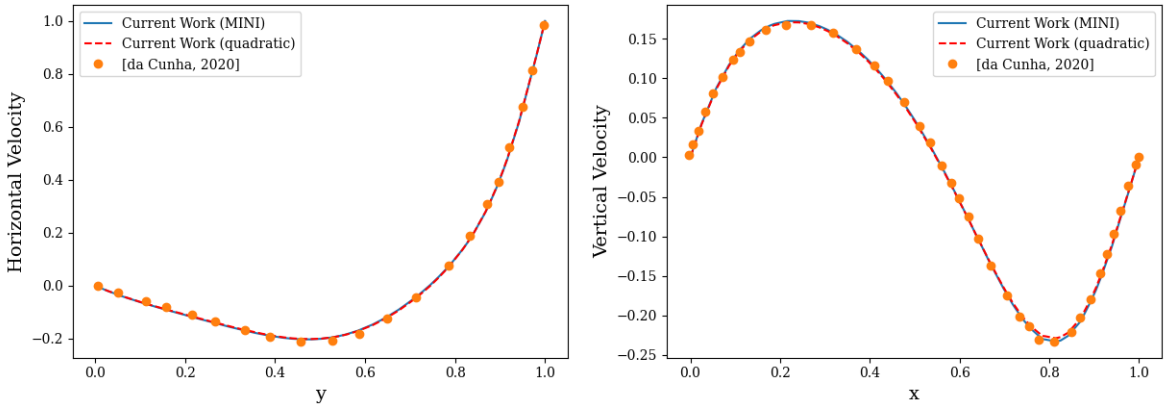

Figure 4: Validation of the lid-driven cavity problem, for velocity components obtained from the central lines crossing the domain, as seen in (da Cunha, 2020).

The result presented is double-validated, since da Cunha (2020) also validates his simulation with the literature, and shows that the implementation in this work was adequate.

5.2 The Expansion with Heat Transfer

Introducing particles' transportation through the domain, using MINI elements, this case study shows the behavior of fluid and solid phases when subjected to an increase in cross section area to the main flow. Figure 5 (a) shows the geometry and the stream lines for $Re = 1000$, $Gr = 0$ and $Ga = 1/Fr^2 = 10^{-4}$. The fluid enters the chamber at null non-dimensional temperature and the three cylinders, at $T = 1.0$, heat up the flow, as shown in Figure 5 (b). The mesh used has 770 elements and 883 vertices.

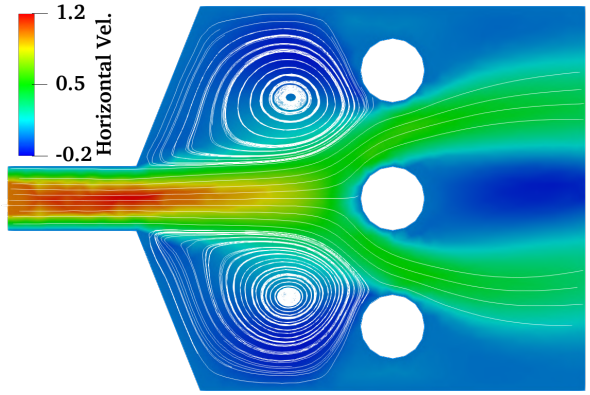

(a) Stream lines in the expansion problem, for $Re = 1000$.

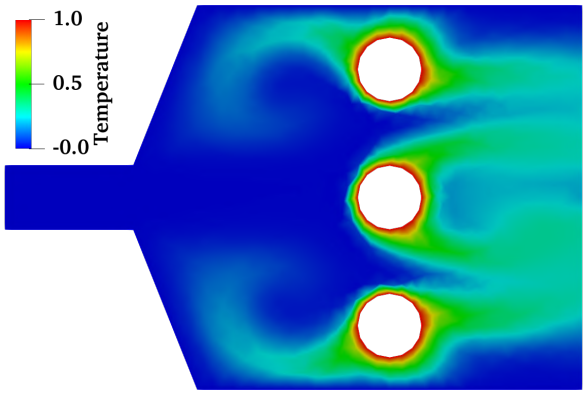

(b) Temperature field in the expansion problem, for $Re = 1000$.

Figure 5: Stream lines and temperature field in the expansion problem, for $Re = 1000$, using the MINI elements in a mesh with 770 elements and 883 vertices.

It is noticeable that temperature field and particles' paths follow the stream lines' behavior, as presented in Figure 6.

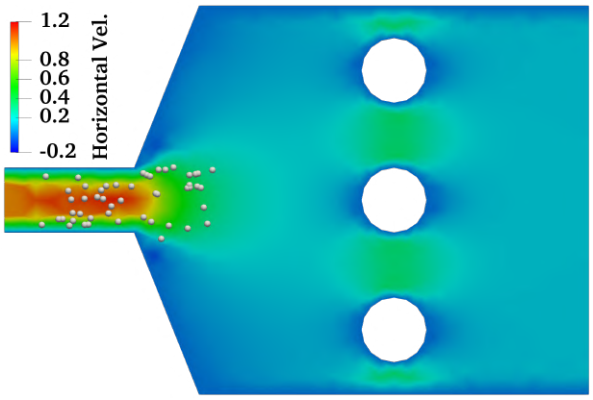

(a) $t = 10$

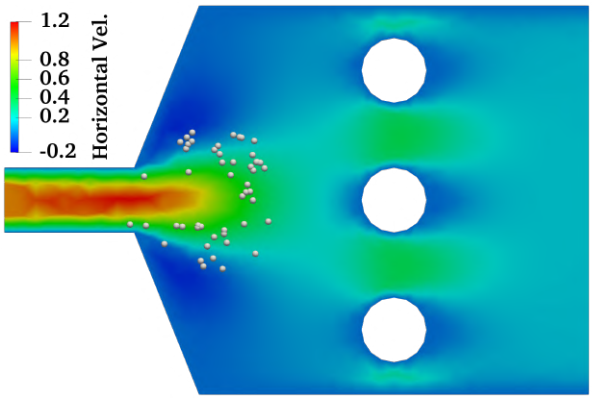

(b) $t = 50$

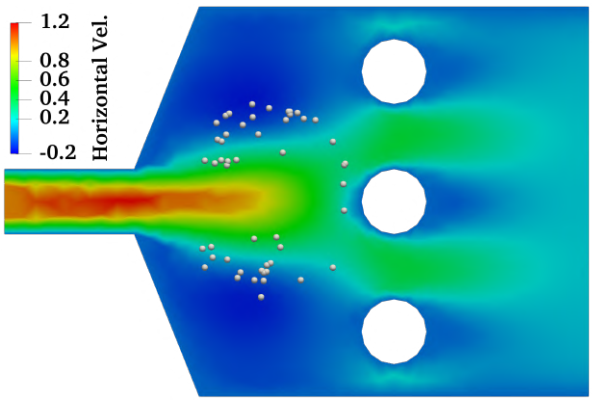

(c) $t = 100$

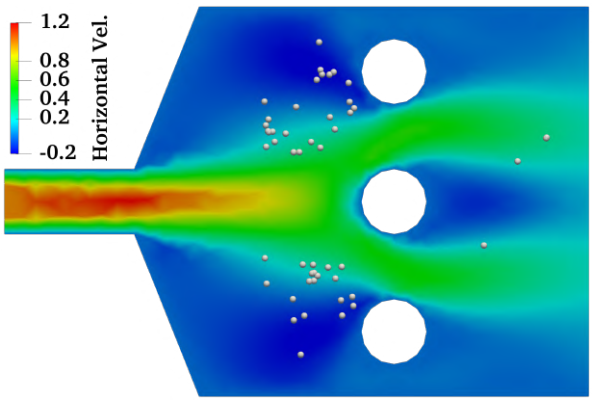

(d) $t = 200$

Figure 6: Particles' motion at different time steps, for $Re = 1000$. (a) $t = 10$, (b) $t = 50$, (c) $t = 100$, (d) $t = 200$.

The sequence shows how light particles end up trapped in the recirculation region and only a few of them get passed through the cylinders. In terms of particle pollution control, that represents an important result as emission to atmosphere may be reduced with a simple mechanism. Also, the Finite Element approach was able to capture the recirculation phenomenon, demonstrated by the stream lines plot, as a result of the high Reynolds number of 1000. Thus, the semi-lagrangian method, with a reasonable time step was able to simulate the expansion, substituting the non linear advective term.

6. CONCLUSION

This work presented a brief literature review on both biofuel scenario and numerical simulation for fluid dynamics, going through studies about renewable sources of energy and how they can substitute fossil ones, as well as numerical

methods to simulate multiphase flows, which is the the aspect observed in emissions resulted from fuel consumption.

The finite element method is used in the Navier-Stokes differential system of equations along with continuity and energy ones. For the material derivative, a semi-Lagrangian approach was used, in order to avoid non-linear terms of the equations. The final result is a linear system of equations for which the variables are the pressure, temperature and velocity points. An Euler-Lagrange methodology is used to calculate the fluid interference in the solid particles, with respect to bouyancy and drag forces.

A first validation of the implemented method is made for the traditional lid-driven cavity problem, comparing results to the ones from the literature. The satisfactory plot of both MINI and quadratic solutions attends the expectations of a simple fluid mechanics problem. Then, an expansion problem with heat transfer associated is analyzed with respect to temperature field and particles' movement, bringing to discussion the importance of recirculation zones, captured by the semi-lagrangian method, in terms of particle emissions, given that most particles end up trapped in the recirculation zones, which are shown in the plotted stream lines.

7. ACKNOWLEDGMENTS

The authors would like to thank the Royal Society-Newton Advanced Fellowship, FAPERJ and CAPES.

8. REFERENCES

Abdelwahed, M., Chorfi, N. and Hassine, M., 2011. "A stabilized finite element method for stream function vorticity formulation of navier-stokes equations". *Electronic Journal of Differential Equations*, Vol. 2017, No. 24, pp. 1–10.

Anjos, G.R., 2007. *Solução do Campo Hidrodinâmico em Células Eletroquímicas pelo Método de Elementos Finitos*. Master's thesis, COPPE/Universidade do Federal do Rio de Janeiro.

Bagai, S., Kumar, M. and Patel, A., 2020. "The four-sided lid driven square cavity using stream function-vorticity formulation". *Journal of Applied Mathematics and Computational Mechanics*, pp. 17–30. doi:10.17512/jamcm.2020.2.02.

Barghi, S.N.S.S., 2015. "Reduction of fine particle emission from a prilling tower using cfd simulation". *Chemical Engineering Research and Design*. doi:http://dx.doi.org/doi:10.1016/j.cherd.2016.01.017.

Batchelor, G.K., 2000. *An Introduction to Fluid Dynamics*. Cambridge University Press, USA.

Borello, D., Rispoli, F. and Venturini, P., 2012. "An integrated particle-tracking impact/adhesion model for the prediction of fouling in a subsonic compressor". *Journal of Engineering for Gas Turbines and Power*, Vol. 134. doi: 10.1115/1.4006840].

Crowe, C.T., Schwarzkopf, J.D., Sommerfeld, M. and Tsuji, Y., 2012. *Multiphase Flows with Droplets and Particles*. CRC Press, USA.

da Cunha, L.H.C., 2020. *Ale Finite Element Method for Simulating Flowswith the Stream Function-Vorticity Formulation*. Master's thesis, Mech. Eng. Program of Universidade do Estado do Rio de Janeiro.

Greifzu, F., Kratzsch, C., Forgber, T., Lindner, F. and Schwarze, R., 2015. "Assessment of particle-tracking models for dispersed particle-laden flows implemented in openfoam and ansys fluent". *Engineering Applications of Computational Fluid Mechanics*, Vol. 10, No. 1, pp. 30–43. doi:10.1080/19942060.2015.1104266.

Hashim, H., Narayanasamy, M., Yunus, N.A., Shiun, L.J., Muis, Z.A. and Ho, W.S., 2016. "A cleaner and greener fuel: Biofuel blend formulation and emission assessment". *Journal of Cleaner Production*, pp. 1–10. doi: http://dx.doi.org/10.1016/j.jclepro.2016.06.021.

Hoffmann, A.C., Åshild Skorpen and Chang, Y.F., 2019. "Positron emission particle tracking and cfd investigation of hydrocyclones acting on liquids of varying viscosity". *Chemical Engineering Science*, Vol. 200, pp. 310–319. doi: https://doi.org/10.1016/j.ces.2019.01.061.

Kim, N., Cho, S. and Min, K., 2015. "A study on the combustion and emission characteristics of an si engine under full load conditions with ethanol port injection and gasoline direct injection". *Fuel*, Vol. 158, pp. 725–732. doi: http://dx.doi.org/10.1016/j.fuel.2015.06.025.

NASA, 2021. "The causes of climate change". URL `https://climate.nasa.gov/causes/`.

Reham, S.S., Masjuki, H.H., Kalam, M.A., Shancita, I., RizwanulFattah, I.M. and Ruhul, A.M., 2015. "Study on stability, fuel properties, engine combustion, performance and emission characteristics of biofuel emulsion". *Renewable and Sustainable Energy Reviews*, Vol. 52, pp. 1566–1579. doi:http://dx.doi.org/10.1016/j.rser.2015.08.013.

Xu, L., Cheng, J.H., Liu, P., Wang, Q., Xu, Z.X., Liu, Q. and Jin-You Shen, L.J.W., 2018. "Production of bio-fuel oil from pyrolysis of plant acidified oil". *Renewable Energy*. doi:10.1016/j.renene.2018.07.012.

Zhang, K., Wang, C.A. and Tan, J.Y., 2018. "Numerical study with openfoam on heat conduction problems in heterogeneous media". *International Journal of Heat and Mass Transfer*, pp. 1156–1162.

Zienkiewicz, O.C. and Taylor, R.L., 2000. *The Finite Element Method - Volume 3*. Wiley.

9. RESPONSIBILITY NOTICE

The authors are solely responsible for the printed material included in this paper.